Journal of Inclusion Phenomena and Macrocyclic Chemistry **35:** 75–84, 1999.

Silver(I) Cation Complexation with 3α,3$'\alpha$-Bis(pyridine-*n*-carboxy) Lithocholic Acid 1,2-Ethanediol Diesters (*n* = 2–4): ^{1}H, ^{13}C and ^{15}N NMR Spectral Studies and Molecular Orbital Calculations

ERKKI KOLEHMAINEN*, JARI TAMMINEN, REIJO KAUPPINEN and JUHA LINNANTO
Department of Chemistry, University of Jyväskylä, P.O. Box 35, FIN-40351 Jyväskylä, Finland

Abstract. Three isomeric molecular clefts: 3α,3$'\alpha$-bis(pyridine-*n*-carboxy) lithocholic acid 1,2-ethanediol diesters (*n* = 2–4) **1–3** have been synthesized and their structures ascertained by ^{1}H, ^{13}C NMR and MALDI TOF MS. Their complex formation with Ag^{+}-cation (added as AgO_3SCF_3) have been investigated by means of NMR and molecular orbital calculations. The coordination behaviour of the silver(I) cation is dependent on the isomerism of the pyridine-*n*-carboxy moiety. In **1** (pyridine-2-carboxylato = picolinato) both NMR and theoretical calculations strongly suggest that the coordination occurs with the lone electron pairs of the pyridine nitrogen and carbonyl oxygen in both of the arms of the molecular cleft separately. In **2** and **3** (pyridine-3-carboxylato = nicotinato and pyridine-4-carboxylato = isonicotinato) where the distance between the pyridine nitrogen and carbonyl oxygen is too large to allow the same type of coordination as in **1**, η^1-complexation with the pyridine ring and carbonyl oxygen of the different arms of the molecular cleft simultaneously is suggested by molecular orbital calculations and supported also by NMR. No Ag^{+}-cation coordination was observed with the 1,2-ethanediol oxygens in **1–3**.

Key words: lithocholic acid, pyridine n-carboxylates, silver(I) cation complexation, ^{1}H, ^{13}C and ^{15}N NMR, MO calculations.

1. Introduction

Bile acids and their conjugates are generally known to possess a specific role in human physiology by solubilizing and emulsifying lipids, lipophilic vitamins, some drugs etc. In addition, some bile acid derivatives are planned to act as suitable drug shuttles for liver specific targeting [1]. In tailoring new hosts capable of specific recognition of guest molecules and ions, bile acids have been shown to possess extraordinarily suitable properties [2, 3]. In our previous studies we have repor-

* Author for correspondence. Phone: +358-14-602670; Fax: +358-14-602501; E-mail: ekolehma@cc.jyu.fi

ted syntheses and NMR spectral characterizations of several cyclic "head-to-tail" macrolides and a cholanophane derived from lithocholic acid (3α-hydroxy-5β-cholan-24-oic acid) [4–9]. Further, we demonstrated by ^{1}H NMR studies that lithocholic acid derived cyclic "head-to-tail" triolides form supramolecular adducts with dicyclopentadienyliron (ferrocene) [10]. In order to tailor bile acid derived hosts suitable for binding of (*d*-block) transition metal cations, addition of nitrogen atom(s) in these structures opens new possibilities also from the heteronuclear NMR point of view. This work is a continuation of our recent study on the syntheses and ^{13}C NMR spectroscopic characterization of bile acid derived molecular clefts [11].

2. Experimental

2.1. COMPOUNDS

Lithocholic acid (3α-hydroxy-5β-cholan-24-oic acid) was 98% product from Aldrich Ltd.

Pyridine-*n*-carboxylic acid chloride: 0.40 g (3.25 mmol) of pyridine-*n*-carboxylic acid and 10 mL of freshly distilled $SOCl_2$ was refluxed for 30 min. After that the excess of thionyl chloride was evaporated under vacuum. The crude product was dissolved in CCl_4 and evaporated to dryness under vacuum. CCl_4 treatment was repeated twice: yield 0.44 g (ca. 100%).

3α,3′α-bis(pyridine-*n*-carboxy) lithocholic acid 1,2-ethanediol diesters **1–3**: A solution of 0.50 g (0.64 mmol) lithocholic acid 1,2-ethanediol diester [8] in 65 mL of sodium-dried toluene was poured into a 0.44 g portion of freshly prepared pyridine-*n*-carboxylic acid chloride. Then 0.4 mL (5 mmol) of pyridine was added and the mixture was kept at 100 °C on an oil bath for 90 h. After that toluene was evaporated under vacuum and the residue was dissolved in $CHCl_3$. The $CHCl_3$-solution was washed with saturated $NaHCO_3$ (4 × 40 mL), water (1 × 40 mL), dried ($MgSO_4$) and evaporated to dryness under vacuum. The crude product was purified by column chromatography (silica gel, ethyl acetate : CH_2Cl_2, 12 : 88): yield in case of **1** 0.11 g (17%), **2** 0.18 g (28%) and **3** 0.12 (19%), respectively. The purities and structures of **1–3** were ascertained by ^{13}C DEPT-135, ^{1}H, ^{13}C NMR, ^{1}H,^{13}C HMQC and MALDI TOF MS. The Ag^{+}-complexation studies have been performed in $CDCl_3$ by saturating the solution with AgO_3SCF_3.

2.2. NMR AND MS

^{1}H, ^{13}C NMR and ^{1}H, ^{13}C HMQC [12, 13] experiments have been run with a Bruker Avance DPX 250 NMR spectrometer equipped with a 5 mm diameter broad band inverse probehead working at 250.13 MHz in ^{1}H and 62.90 MHz in ^{13}C or a Bruker Avance DRX 500 NMR spectrometer equipped with a 5 mm diameter broad band direct probehead working at 500.13 MHz in ^{1}H and 125.77 MHz in ^{13}C. ^{1}H,^{15}N HMBC [14] experiments with *z*-gradient selection have been run with

a Bruker Avance DRX 500 NMR spectrometer equipped with a 5 mm diameter broad band inverse probehead working at 500.13 MHz in ^{1}H and 50.69 MHz in ^{15}N. The ^{13}C NMR chemical shift assignments are based on our previous studies [9], ^{13}C DEPT-135 and ^{1}H, ^{13}C HMQC experiments. The complete lists of the acquisition and processing parameters are available from E.K. on request. MALDI TOF MS-measurements have been done by a Bruker Polymer TOF equipment working in the reflectron mode and with a N_2-laser.

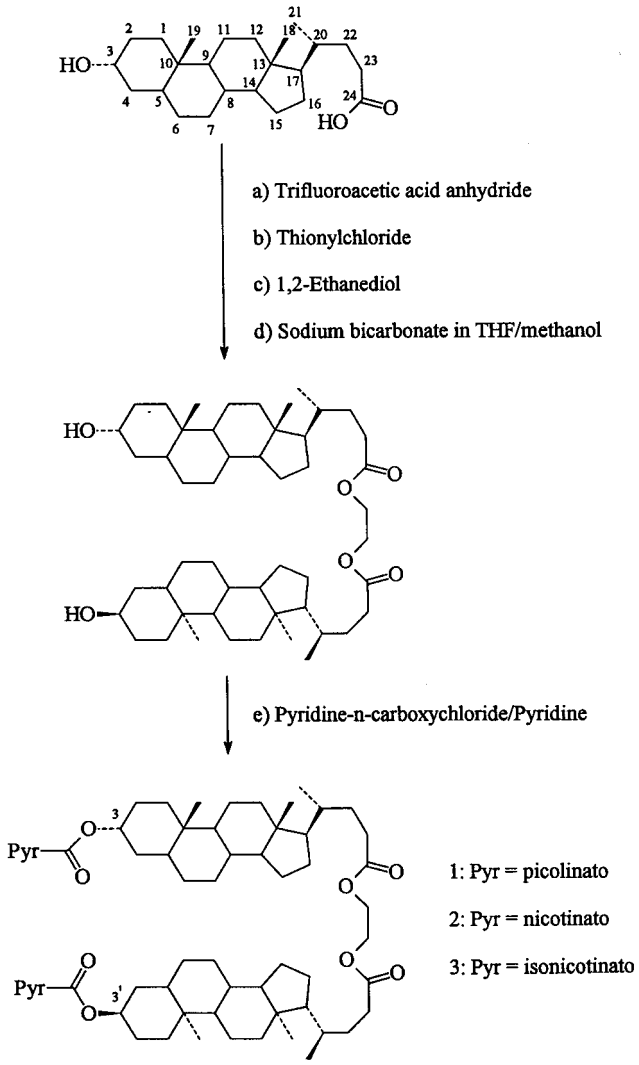

Scheme 1.

2.3. MOLECULAR ORBITAL CALCULATIONS

The geometries of the ligands (**1**, **2**, and **3**) were fully optimized at the PM3 [15] level on a Silicon Graphics O2 workstation by using SPARTAN software [16]. The optimizations of the substructures of ligands (containing only the pyridine-*n*-carboxy and cyclohexyl A from the bile acid) with and without Ag^+-cation at *ab initio* level were then continued keeping the rest of the molecule fixed on a Silicon Graphics Origin 200 workstation at the HF/3-21G(d) level by using the Gaussian 94 program [17]. Finally, the geometries of the optimized substructures were used in computing the ^{13}C NMR chemical shift changes caused by silver(I) complexation in **1**–**3**.

3. Results and Discussion

The synthetic route of compounds **1**–**3** is described in Scheme 1. ^{13}C NMR chemical shifts of compounds **1**–**3** and their Ag^+-complexes are given in Table I. The ^1H, ^{13}C HMQC contour map of **1** is shown in Figure 1. Tables II and III contain the most significant ^1H and ^{13}C NMR chemical shift changes of **1**–**3** caused by the addition of AgO_3SCF_3. The calculated ^{13}C NMR chemical shift changes in the pyridine-*n*-carboxy-moieties of **1**–**3** caused by the addition of AgO_3SCF_3 are also catalogued in Table III.

As can be seen in Table II the most significant ^1H NMR chemical shift changes associated with AgO_3SCF_3 addition occur in the pyridine protons of **1**. The same is true also for the ^{13}C NMR chemical shift changes in **1**, when compared with the other isomers **2** and **3** (Table III). These findings suggest that there exist some differences in complexation properties between the species **1** vs. **2** and **3**. In order to clarify the experimental results, some molecular orbital calculations have also been done for the ligands themselves and their Ag^+-complexes.

Energetically the most favoured conformation of the Ag^+-complex of **1** is described in Figure 2. A rotation of the pyridine moiety has a minimal influence on the energy of the ligand itself but in its Ag^+-complex only one conformation is strongly preferred for steric reasons. Further, theoretical calculations show that the Ag^+-cation is coordinated with the pyridine nitrogen and carbonyl oxygen simultaneously. In **2** and **3** this kind of coordination of the silver cation inside one arm of the molecular cleft is not possible. In order to satisfy the coordination demands of the silver(I) cation intramolecularly, the complexes have to adopt different conformational states in comparison with **1** as described in Figures 3 and 4. In these cases energetically the most preferred coordinated structures with silver(I) cation are obtained when it is simultaneously coordinated with the nitrogen of the pyridine ring of one arm and the carbonyl oxygen of the other arm. This kind of η^1-complexation where the silver(I) cation is not located in the plane of the aromatic ring was recently reported by Mascal *et al.*, based on single crystal X-ray analysis [18]. Because the nitrogen lone electron pair is not so strongly involved in the coordination in these arrangements as in **1**, these models also explain why the

Table I. ^{13}C NMR chemical shifts (ppm from $CDCl_3$, δ = 77.0 ppm) of isomeric 3α,3′α-bis(pyridine-*n*-carboxy) lithocholic acid 1,2-ethanediol diesters **1**–**3** and their Ag^+-complexes

	δ (^{13}C)/ppm					
Carbon	**1**	**2**	**3**	**1 + Ag**	**2 + Ag**	**3 + Ag**
1	35.14	34.94	35.02	34.81	34.99	34.92
2[a]	26.54	26.63	26.66	26.40	26.51	26.48
3	76.06	75.62	76.16	78.16	76.56	76.95
4[b]	32.18	32.22	32.25	31.99	32.12	32.07
5	42.03	41.88	41.97	41.84	41.97	41.92
6[a]	27.05	26.95	27.04	26.88	27.02	26.97
7[a]	26.32	26.25	26.36	26.22	26.26	26.28
8[c]	35.81	35.74	35.84	35.67	35.80	35.78
9	40.27	40.43	40.56	40.42	40.38	40.46
10	34.65	34.55	34.65	34.49	34.61	34.57
11	20.80	20.80	20.91	20.77	20.86	20.87
12	40.16	40.04	40.17	40.00	40.00	40.06
13	42.74	42.68	42.79	42.65	42.71	42.73
14[d]	56.49	56.38	56.53	56.32	56.26	56.37
15	24.20	24.10	24.21	24.08	24.17	24.17
16	28.17	28.08	28.20	28.07	28.12	28.12
17[d]	55.99	55.93	56.08	55.96	55.90	55.93
18	12.03	11.98	12.09	11.97	12.02	12.04
19	23.21	23.25	23.34	23.18	23.28	23.25
20[c]	35.33	35.24	35.36	35.21	35.25	35.23
21	18.24	18.19	18.30	18.20	18.22	18.22
22[b]	31.11	31.02	31.14	31.05	31.11	31.08
23[b]	30.89	30.84	30.95	30.83	30.93	30.93
24	173.93	173.83	173.95	173.91	173.92	173.96
25	62.03	61.94	62.06	61.98	62.02	62.06
CO	164.74	164.57	164.50	163.9	163.35	162.91
1′	148.67	126.70	138.32	145.11	128.21	140.74
2′	–	150.58	122.96	–	151.74	124.53
3′	149.80	–	150.30	152.1	–	151.69
4′	126.64	152.84	–	129.11	154.21	–
5′	136.91	123.21	150.30	139.93	124.67	151.69
6′	125.10	137.06	122.96	126.13	139.41	124.53

[a–d] Assignments may be interchanged.

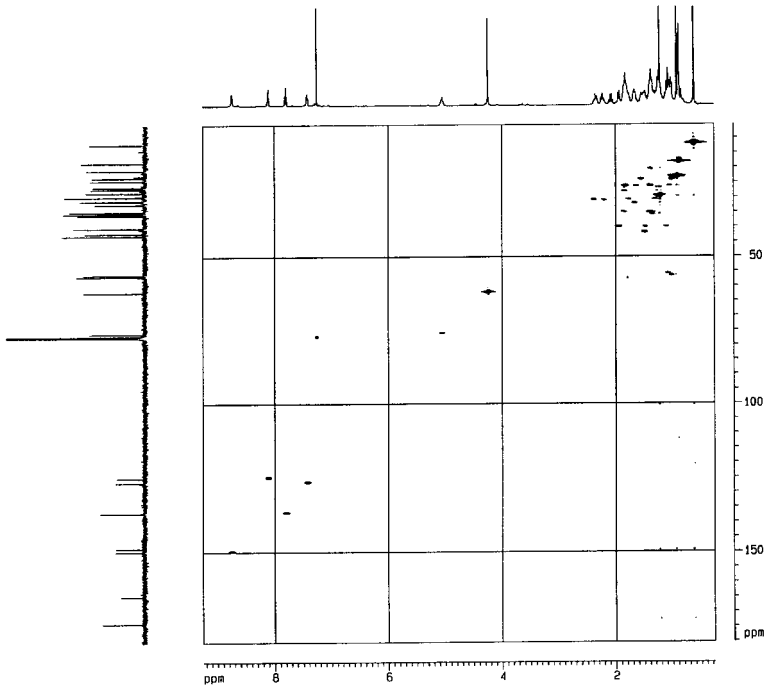

Figure 1. ^{1}H, ^{13}C HMQC countour map of **1** measured in $CDCl_3$ at 30 °C.

Table II. ^{1}H NMR chemical shift changes caused by AgO_3SCF_3 in **1–3**

Proton	$\Delta\delta(^{1}H)^{a}$/ppm		
	1	**2**	**3**
3β	0.00	0.02	0.00
2′	–	0.02	0.14
3′	0.23	–	0.08
4′	0.36	0.19	–
5′	0.30	0.17	0.08
6′	0.19	0.16	0.14

carbonyl carbon chemical shifts are influenced more in **2** and **3** than in **1** associated with the silver(I) cation complexation. This conclusion is also supported by the inverse effects observed in the *ipso*-carbon C-1′ chemical shifts in **1** vs. **2** and **3**. As can be seen in Table III, the *ab initio* MO calculations at the HF/3-21G(d) level produce $\Delta\delta(^{13}C)$-values which are qualitatively in agreement with the exper-

Table III. Experimental and calculated ^{13}C NMR chemical shift changes caused by AgO_3SCF_3 in **1**–**3**

	$\Delta\delta(^{13}C)$[a]/ppm					
	1		**2**		**3**	
Carbon	Exp.	Calc.	Exp.	Calc.	Exp.	Calc.
3	+2.10	+0.71	+1.04	+0.50	+0.79	+0.45
CO	−0.84	0.54	−1.22	−0.62	−1.59	−1.08
1′[b]	−3.56	−0.56	+1.51	+0.91	+2.42	+0.90
2′	–	–	+1.16	+0.83	+1.57	+0.53
3′	+2.30	+0.75	–	–	+1.39	+0.47
4′	+2.47	+0.74	+1.34	+0.84	–	–
5′	+3.02	+0.78	+1.46	+0.87	+1.39	+0.49
6′	+1.03	+0.58	+2.35	+1.15	+1.57	+0.54

[a] Shift change is positive when silver complexation causes deshielding.
[b] Carboxy bearing pyridine carbon C-1′.

Figure 2. Optimized structure of the Ag^+-complex of **1**.

imental chemical shift changes. Unfortunately, for the silver(I) cation there is not any better parameterization available than used now.

To get additional evidence for the above suggestion on the different complexation behavior between **1** vs. **2** or **3**, ^1H,^{15}N HMBC experiments with *z*-gradient selection were also performed for **1** and **2**. Both ligands gave clear cross peaks at almost the same ^{15}N chemical shift values being −69.6 ppm for **1** and −69.1 ppm for **2** from the shift of neat nitromethane $\delta(^{15}N) = 0.0$ ppm. These values are in accord with that of pyridine-2-carboxylic acid, $\delta(^{15}N) = -65.4$ ppm, measured in DMSO [19]. In contrast to the values of the ligands **1** and **2**, their Ag^+-complexes

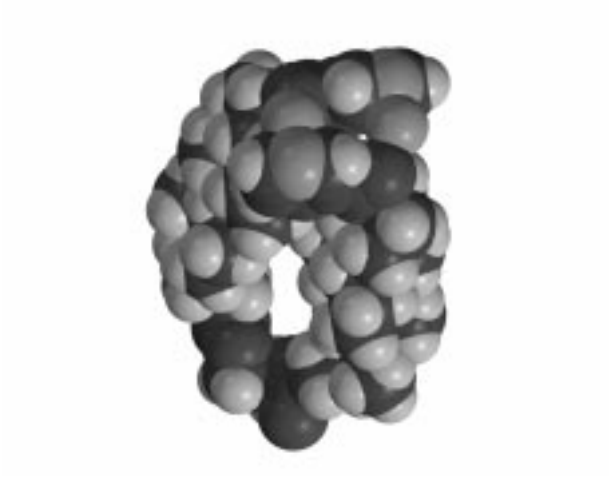

Figure 3. Optimized structure of the Ag^+-complex of **2**.

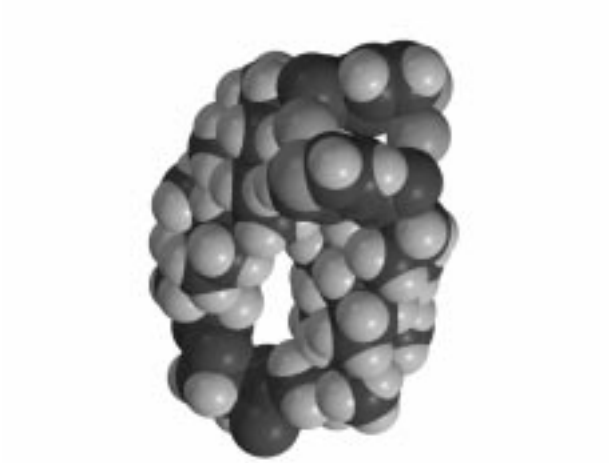

Figure 4. Optimized structure of the Ag^+-complex of **3**.

gave clearly different ^{15}N chemical shifts being −111.8 ppm for **1 + Ag** and −119.2 ppm for **2 + Ag**, respectively. In Figure 5 we show a partial plot of the z-GS ^{1}H, ^{15}N HMBC contour map of **2 + Ag** showing a clear cross-peak between H-2′ and pyridine nitrogen N-3′ transmitted by ^{2}J(H-2′, N-3′) during a 50 ms evolution time. Unfortunately, as far as we know there does not exist any reference data on ^{15}N NMR chemical shifts on Ag^+-pyridine complexes. In any case the observed shift is upfield as in the case of a protonation of pyridine nitrogen [20].

An interesting feature was observed in the ^{1}H NMR of **1–3**. At 30 °C the ^{1}H NMR resonances of protons adjacent to the pyridine nitrogen are strongly broadened. This can be explained as due to a dynamic equilibrium between the

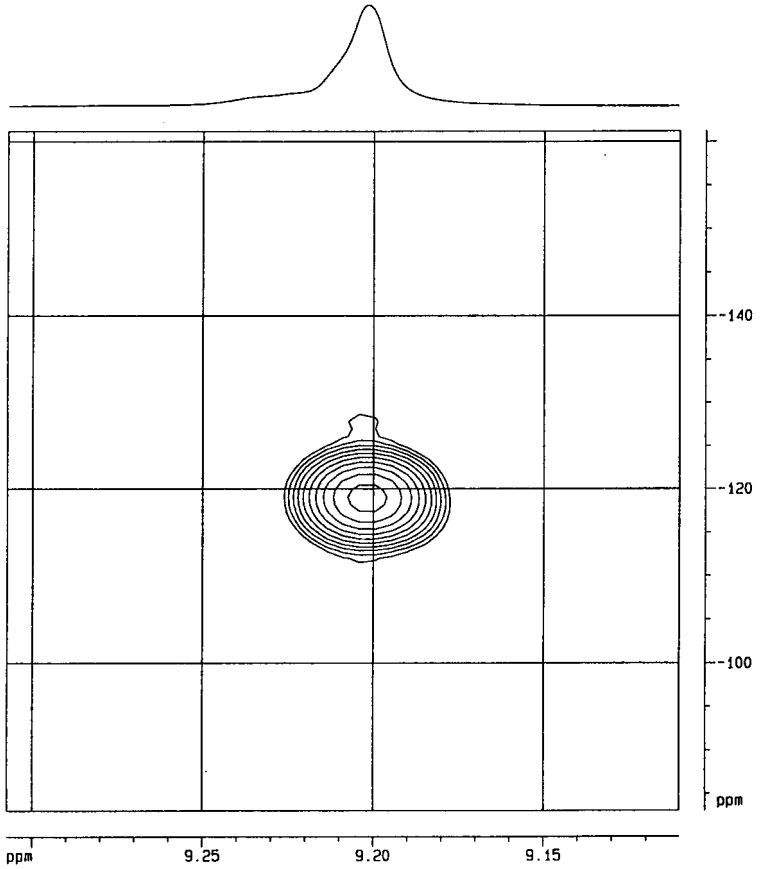

Figure 5. A partial plot of the *z*-GS $^{1}H,^{15}N$ HMBC contour map of the Ag^{+}-complex of **2** measured in $CDCl_3$ at 30 °C.

free and complexed pyridine nitrogen with solvent ($CDCl_3$) molecules because at −50 °C the signals were sharpened. A clear improvement in the resolution of these signals was also achieved at 30 °C by addition of traces of silvertriflate to the sample. This means that the association tendency of silver cation with these structures is predominant hindering the influence by the solvent molecules. The association constants between Ag^{+}-cation and these molecular clefts and the ^{109}Ag NMR studies of these complexes are in progress and will be published later.

4. Conclusions

Multinuclear magnetic resonance spectroscopic methods are a powerful tool in clarifying the transition metal coordination with nitrogen containing bile acid derived molecular clefts prepared in this work. In fact, these methods are the only efficient way to approach this complex topic because any attempts to crystallize these

structures suitable for single crystal X-ray analysis failed. The present topic has remarkable potentials regarding the studies of catalysis, mimicking biochemically interesting systems, tailoring molecular hosts for specific recognition of transition metal cations, transition metal coordination chemistry etc.

Acknowledgements

We are grateful to Assoc. Prof. P. Vainiotalo and M.Sc. J. Nuutinen (Univ. Joensuu, Finland) for running the MALDI TOF mass spectra. The Academy of Finland has financially supported this work, which is also gratefully acknowledged.

References

1. G. Wess, W. Kramer, A. Enhsen, H. Glombik, K.-H. Baringhaus, K. Bock, H. Kleine, and W. Schmitt: *Tetrahedron Lett*. **34**, 819 (1993) and references cited therein.
2. A. P. Davis: *Chem. Soc. Rev*. **22**, 243 (1993) and references cited therein.
3. A. P. Davis, J. J. Perry, and R. S. Wareham: *Tetrahedron Lett*. **39**, 4569 (1998) and references cited therein.
4. E. Kolehmainen, M. Kaartinen, R. Kauppinen, J. Kotoneva, K. Lappalainen, P. T. Lewis, R. Seppälä, J. Sundelin, and V. Vatanen: *Magn. Reson. Chem*. **32**, 441 (1994).
5. K. Lappalainen, E. Kolehmainen, M. Kaartinen, R. Kauppinen, R. Seppälä, and V. Vatanen: *Magn. Reson. Chem*. **32**, 786 (1994).
6. K. Lappalainen, E. Kolehmainen, and D. Šaman: *Spectrochim. Acta, Part A* **51**, 1543 (1995).
7. K. Lappalainen, E. Kolehmainen, and J. Kotoneva: *Magn. Reson. Chem*. **34**, 316 (1996).
8. E. Kolehmainen, J. Tamminen, K. Lappalainen, T. Torkkel, and R. Seppälä: *Synthesis* 1082 (1996).
9. K. Lappalainen: Ph.D. Thesis, Research Report No. 62, Department of Chemistry, University of Jyväskylä (1997) and references cited therein.
10. K. Lappalainen and E. Kolehmainen: *Liebigs Ann./Recueil* 1965 (1997).
11. J. Tamminen, K. Lappalainen, K. Laihia, P. Mänttäri, H. Salo, and E. Kolehmainen: *Magn. Reson. Chem*. **37**, 163–165 (1999).
12. A. Bax, R. H. Griffey and B. L. Hawkins: *J. Magn. Reson*. **55**, 301 (1983).
13. A. Bax and S. Subramanian: *J. Magn. Reson*. **67**, 565 (1986).
14. A. Bax and M.F. Summers: *J. Am. Chem. Soc*. **108**, 2093 (1986).
15. J. J. P. Stewart: *J. Comput. Chem*. **10**, 209 (1989).
16. SPARTAN, Version 5.0.2, Wavefunction Inc., Irvine, CA, 1991–1997.
17. M. J. Frisch, G. W. Trucks, H. B. Schlegel, P. M. W. Gill, B. G. Johnson, M. A. Robb, J. R. Cheeseman, T. Keith, G. A. Petersson, J. A. Montgomery, K. Raghavachari, M. A. Al-Laham, V. G. Zakrzewski, J. V. Ortiz, J. B. Foresman, J. Cioslowski, B. B. Stefanov, A. Nanayakkara, M. Challacombe, C. Y. Peng, P. Y. Ayala, W. Chen, M. W. Wong, J. L. Andres, E. S. Replogle, R. Gomperts, R. L. Martin, D. J. Fox, J. S. Binkley, D. J. Defrees, J. Baker, J. P. Stewart, M. Head-Gordon, C. Gonzalez, and J. A. Pople: GAUSSIAN 94, Revision B.1, Gaussian Inc., Pittsburgh PA, 1995.
18. M. Mascal, J. Hansen, A. J. Blake, and W.-S. Li: *J. Chem. Soc., Chem. Commun.* 355 (1998).
19. W. Städeli and W. von Philipsborn: *Org. Magn. Reson*. **15**, 106 (1981).
20. R. O. Duthaler and J. D. Roberts: *J. Am. Chem. Soc*. **100**, 4969 (1978).